NASA Technical Paper 1101

Significant Initial Results From the Environmental Measurements Experiment on ATS-6

T. A. Fritz, J. P. Corrigan, et al.

DECEMBER 1977

NASA

NASA Technical Paper 1101

Significant Initial Results From the Environmental Measurements Experiment on ATS-6

T. A. Fritz, J. P. Corrigan, et al.
Goddard Space Flight Center
Greenbelt, Maryland

All measurement values are expressed in the International System of Units (SI) in accordance with NASA Policy Directive 2220.4, paragraph 4.

SIGNIFICANT INITIAL RESULTS FROM THE ENVIRONMENTAL MEASUREMENTS EXPERIMENT ON ATS-6

BY

T. A. Fritz
Space Environment Laboratory, NOAA
Boulder, Colorado

C. W. Arthur
Institute of Geophysics and Planetary Physics and
Dept. of Geophysics and Space Physics, UCLA
Los Angeles, California

J. B. Blake
The Aerospace Corporation
Los Angeles, California

P. J. Coleman, Jr.
Institute of Geophysics and Planetary Physics and
Dept. of Geophysics and Space Physics, UCLA
Los Angeles, California

J. P. Corrigan
Goddard Space Flight Center
Greenbelt, Maryland

W. D. Cummings
Physics Dept., Grambling State Univ.
Grambling, Louisianna

S. E. DeForest
Physics Dept., Univ. of Alabama
Huntsville, Alabama

K. N. Erickson
School of Physics and Astronomy, Univ. of Minnesota
Minneapolis, Minnesota
Dept. of Physics, Augsburg College
Minneapolis, Minnesota

A. Konradi
Johnson Space Center, NASA
Houston, Texas

W. Lennartsson
Marshall Space Flight Center, NASA
Huntsville, Alabama

A. J. Masley
Aerojet ElectroSystems Co.
Azusa, California

B. H. Mauk
Dept. of Physics, UCSD
LaJolla, California

C. E. McIlwain
Dept. of Physics, UCSD
LaJolla, California

R. L. McPherron
Institute of Geophysics and Planetary Physics and
Dept. of Geophysics and Space Physics, UCLA
Los Angeles, California

G. A. Paulikas
The Aerospace Corporation
Los Angeles, California

K. A. Pfitzer
McDonnell-Douglas Astronautics Co.
Huntington Beach, California

D. L. Reasoner
Marshall Space Flight Center, NASA
Huntsville, Alabama

P. R. Satterblom
McDonnell-Douglas Astronautics Co.
Huntington Beach, California
Celesco Industries
Costa Mesa, California

S. Y. Su
Lockheed Electronics Co.
Houston, Texas

R. J. Walker
School of Physics and Astronomy, Univ. of Minnesota
Minneapolis, Minnesota

E. C. Whipple, Jr.
Dept. of Physics, UCSD
LaJolla, California

B. Wilken
Max Planck Institute for Aeronomy
3411 Lindau/Harz, West Germany

J. R. Winckler
School of Physics and Astronomy, Univ. of Minnesota
Minneapolis, Minnesota

CONTENTS

SIGNIFICANT INITIAL RESULTS FROM THE ENVIRONMENTAL MEASUREMENTS EXPERIMENT ON ATS-6

INTRODUCTION

The NASA Applications Technology Satellite (ATS-6) was launched into a geostationary orbit on May 30, 1974, carrying into orbit a comprehensive set of instruments designed to study the geosynchronous environment. The satellite is a nonspinning three-axis stabilized platform located at 94°W longitude for the first year of operation. During May 1975, ATS-6 was transferred to 35°E longitude. The science package, called the Environmental Measurements Experiments (EME), has been described in detail in Volume AES-11, no. 6 of the Institute of Electrical and Electronics Engineers *IEEE Transactions of Aerospace and Electronic Systems*. (A sketch of the spacecraft appears later in this document in figure 14.) Briefly, the EME is composed of six particle instruments that are able to determine the particle distribution function for electrons and ions over a range in energy from less than 1 electron volt (eV) to greater than 100 million electron volts, a range of over eight orders of magnitude in energy. In addition, a sensitive, low noise, triaxial fluxgate magnetometer is capable of providing measurements of the local magnetic field and its variations.

The purpose of this document is to present significant initial results returned by these EME instruments owing to their unique design and/or operational characteristics. The presentations in this paper are brief and will be followed by comprehensive papers when additional data analysis is performed by the individual experimenters. Data presented herein are from the first 6 months of operations of the EME experiments at 94°W longitude.

The paper begins with a discussion of the characteristics of the main geomagnetic field 10° above the magnetic equator at a geostationary distance. The magnetic field and particle signatures of field-aligned currents are then discussed, followed by a discussion of the composition and temperature of the plasmasphere. A series of observations of correlated periodic variations in the magnetic field and particles are presented that cover variations with periods from a few seconds to a few weeks. Brief sections then follow about the role of heavy ions, "typical" particle-energy spectra, and the role of spacecraft charging in the geosynchronous environment.

INCLINATION OF THE MAGNETIC FIELD AT ATS-6

The University of California at Los Angeles (UCLA) magnetometer on ATS-6 (Reference 1) consists of an orthogonal array of three fluxgate sensors aligned with the body axes of the spacecraft. The instrument has a dynamic range of ±512γ with a resolution of 1/16γ. The

root mean square (rms) noise in the bandwidth from 10^{-3} to 1 Hz is 85 mγ. The direct current (dc) field of the spacecraft is small; the components perpendicular to the Earth pointing axis are less than 2γ. Particle measurements indicate that the third component of the spacecraft field is also small (Reference 2).

For the purpose of geophysical studies, the magnetometer data are transformed from the local body system to a geophysical coordinate system, called Dipole VDH. This coordinate system and the typical magnetic field geometry at midnight are shown in figure 1. For the first year, ATS-6 was located on the geographic equator approximately 10° above the magnetic equator. Field lines through the satellite pass through the magnetic equator at distances (L values) greater than 6.6 Earth radii. The H-axis of the dipole coordinate system is antiparallel to the Earth's dipole axis. The D-axis is orthogonal to a plane defined by H and a radius vector through the spacecraft; V completes the right-hand system such that V X D = H; V points away from the Earth parallel to the magnetic equator. At times, it is convenient to display the magnetic field data in spherical polar coordinates rather than the V, D, H system. In such cases B $_{TOTAL}$ is the field magnitude, θ the polar angle with respect to the Dipole H-axis, and ϕ the azimuthal angle measured in the VD plane positive eastward from V towards D.
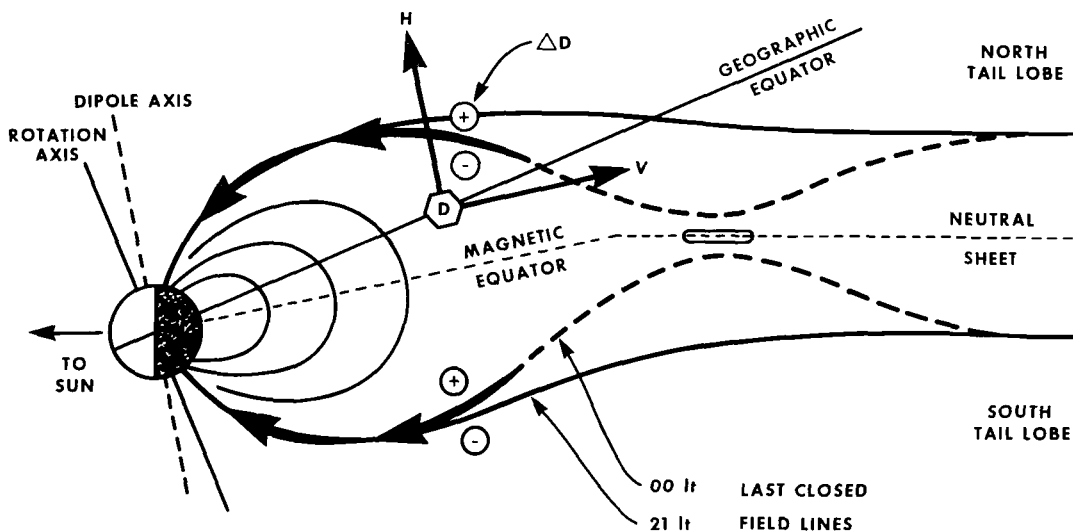

Figure 1. Orientation of the Dipole VDH system at ATS-6, showing
the magnetic perturbations of field-aligned currents near midnight at summer solstice.

Spherical polar coordinates are particularly useful in illustrating a surprising feature of the magnetic field at the location of ATS-6. As can be seen in figure 2, the mean field at local noon is tilted approximately 30° to the dipole axis and has a magnitude of about 135γ.
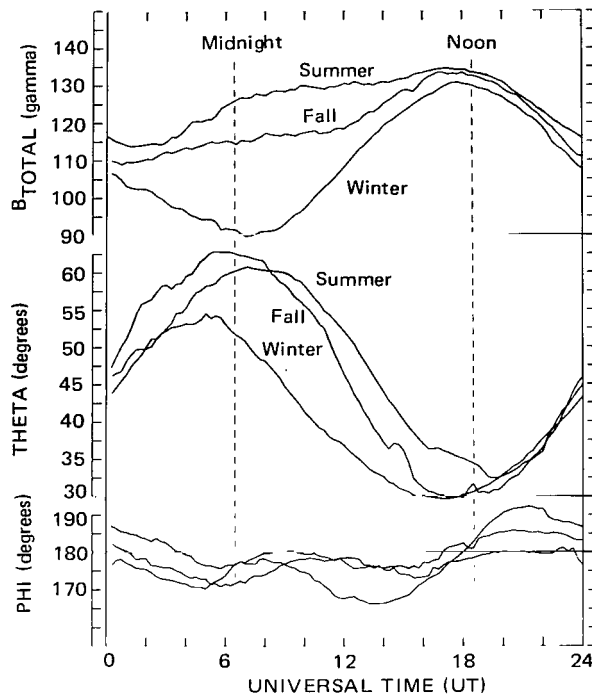
2

Figure 2. Seasonal dependences of the mean magnetic
field at ATS-6.

In a dipole field, these values would be 29° and 112.6γ. Early models of the magnetic field (Reference 3) predicted that values should be 21° and 147γ. These predictions are based on the physical notion that the solar wind compresses the day-side magnetosphere, increasing the field strength at synchronous orbit, and simultaneously flattening the field lines against the dipole axis. However, the observations clearly show that the tilt of the field is larger and the field strength, smaller, than predicted by such a model.

The differences between the ATS-6 observations and these early models can be explained if one assumes that there is significant plasma within the magnetosphere. Off the magnetic equator, such plasma would decrease the field strength and tilt the field away from the dipole axis. Since early models of the magnetopause currents neglected internal plasma, it is not surprising that their predications are in error.

More recent models of the magnetospheric magnetic field do include the effects of internal plasma. For example, Pfitzer (Reference 4) has used the distributed current model of Olson and Pfitzer (Reference 5) to predict the field at ATS-6. According to the predictions, the expected values of tilt and field strength at local noon are 35° and 115γ, respectively. Comparing these with the observations, particularly of the field magnitude, the authors conclude that the currents in the Olson-Pfitzer model are slightly too strong to correspond to average conditions at synchronous orbit.

3

Another surprising characteristic of the mean field at ATS-6 can be seen in figure 2 at local midnight; that is, the obvious seasonal dependence of tilt and magnitude. The winter tilt at midnight is 10° less than the summer tilt, while field magnitude is 35γ less. These observations suggest that the surface of magnetic symmetry at synchronous orbit does not lie in the magnetic equator at the solstices. However, because of a 1.54° tilt of the ATS-6 orbit relative to the geographic equator, this cannot be unambiguously demonstrated.

FIELD-ALIGNED CURRENTS

Recent observations have firmly established that field-aligned currents connect the magnetosphere and the auroral ionosphere. (See, for example, a review by Anderson and Vondrak (Reference 6)). These observations suggest that such currents can be divided into two classes: those that are associated with steady magnetospheric convection and are continuously present, and those that are associated with substorms and are only transiently observed. Convection currents are frequently seen in deep space by eccentric orbiting spacecraft. For example, Sugiura (Reference 7) has used the perturbations due to field-aligned currents to map the night-side boundary of the polar cap.

The transient effects of substorm currents have been more difficult to identify in space. Since a portion of the convection current system flows on the boundary of the plasma sheet, movement of this boundary during substorms can move these currents across a spacecraft. Whether additional current associated with the substorm is flowing on this boundary cannot be unambiguously determined.

Magnetic Effects of Substorm-Associated Field-Aligned Currents

Using data from the ATS-1 satellite at synchronous orbit, Coleman and McPherron (Reference 8) have reported transient azimuthal magnetic field variations during substorms. However, since the ATS-1 spacecraft is located very near the magnetic equator, it is difficult to explain why such magnetic perturbations should be observed. As is easily seen by symmetry arguments, azimuthal effects of field-aligned currents connected to both northern and southern auroral zones ought to cancel at the magnetic equator. At the location of the ATS-6 spacecraft, however, the azimuthal effects of field-aligned currents ought not to cancel.

Examination of daily magnetograms from the ATS-6 spacecraft unambiguously shows the effects of substorm-associated field-aligned currents. These effects are identical to those seen on the ground in the northern hemisphere at mid- and sub-auroral latitudes. Premidnight transient deviations in the azimuthal field are positive, while postmidnight they are negative. This fact is particularly clear in the statistical results shown in figure 3. In this figure, successive traces show the percentile lines of the distribution functions for the azimuthal component (Dipole D). Ten percent of the time, the observed D-component falls below the bottom trace and 10 percent of the time, above the top trace. It is apparent that perturbations from the median are positive premidnight and negative postmidnight.
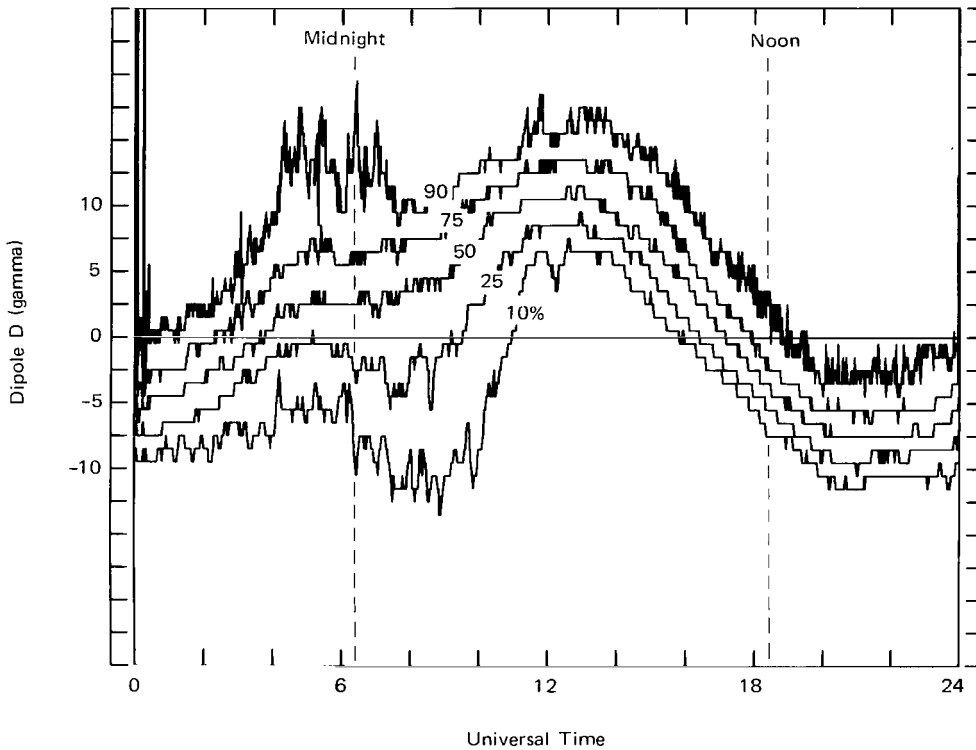
Figure 3. Statistical behavior of the magnetic field at ATS-6 near the summer solstice, 1974.

These observations are entirely consistent with accepted models of substorms and field-aligned currents. In a model proposed by McPherron et al. (Reference 9), the tail current is short-circuited during the substorm expansion phase. Current flows down field lines in the postmidnight sector, westward along the auroral oval, and upward premidnight. As can be seen by examination of figure 1, the effects of this current are the same as is actually observed.

Particle Measurements Associated with Field-Aligned Currents

In the equatorial magnetosphere, the ATS-6 satellite was the first to observe intense beams of 1- to 10-keV electrons traveling parallel to the local magnetic field (Reference 2). Figure 4 shows a spectrum of such a beam taken on June 16, 1974 very near local midnight using the University of California, San Diego (UCSD) Auroral Particles Experiment. The upper trace of the figure was taken with an electrostatic analyzer which is mechanically rotated, and the aperture of which often passed close to the local magnetic field; the

5

lower trace was taken from a similar analyzer sweeping in a direction nominally perpendicular to the field. The parallel spectrum (showing particles moving northward) is considerably enhanced in the 3- to 10-keV energy region relative to the perpendicular spectrum. This enhancement typically falls off markedly for pitch angles greater than 15°. The intense beams seem to occur only within the first 10 minutes after the onset of a hot plasma injection associated with a magnetic substorm.
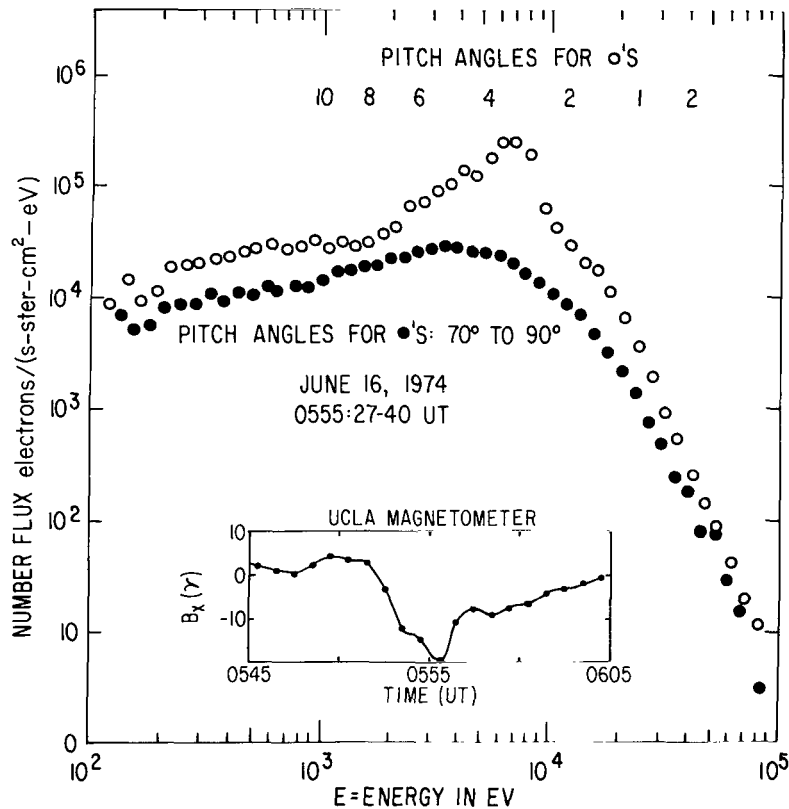

Figure 4. Comparison of electron spectra perpendicular and near-parallel (northward) to the magnetic field taken by UCSD electrostatic analyzers showing a strong field-aligned flux distribution. The insert shows a perturbation in the eastward component of the local magnetic field (measured by the UCLA magnetometer) indicating that the parallel fluxes carry a current.

The insert to figure 4 shows a 20-minute segment of the eastward component (nearly equivalent to the dipole D-component) of the local magnetic field taken with the onboard University of California, Los Angeles (UCLA) magnetometer. The figure, which is typical of many such events, shows that a negative spike in the eastward component is coincident with the occurrence of the parallel fluxes of electrons, indicating that the fluxes

6

are contributing to currents flowing along the magnetic field. Although the origin and destiny of the parallel electrons are as yet unknown, consideration of the total energy and number of particles transported guarantees that they must play an important role in key magnetospheric processes. In particular, these particles may be associated with the initial brightening of auroral arcs.

THE UNEXPECTED EXISTENCE OF A WARM PLASMA IN THE REGION OF THE PLASMASPHERIC BULGE

ATS-6 has observed enhancements in low-energy (warm) plasma (2 to 30 eV) occurring predominantly in the late afternoon and dusk region of the equatorial magnetosphere. These observations are particularly significant because of their possible association with the plasmasphere. One such event is shown in the flux spectrum (ions only) and pitch-angle distribution plots in figures 5a and 5b. The flux spectrum was taken at the peak of the ion pitch-angle distribution. These data, from the UCSD electrostatic analyzers, were taken on August 20, 1974. Figure 5a shows a quasi-Maxwellian ion distribution with a temperature between 5 and 20 eV. Figure 5b shows that the distribution for both ions and electrons is peaked at smaller pitch angles, and that the ions display a significant loss cone (suggesting that these ions have been around for some time rather than freshly injected). This class of low-energy events often shows field-aligned anisotropies, but isotropic distributions, as well as distributions indicative of flows perpendicular to the magnetic field, have also been observed.

The local time (LT) distribution of encounters with this low-energy ion plasma is shown in figure 5c. In this figure, the angular coordinate is local time and the radial component is the probability of occurrence in each 10-minute sector of local time. For these events, densities ranged from 1 to 10 ions/cm^3. Typical temperatures were in the range of 5 to 10 eV, but were often observed to be as low as 2 eV and as high as 30 eV. Coincident electron plasma temperatures tended to be lower. (Low-energy electron measurements suffer from photoelectron contamination, however.)

Were it not for the high temperatures, one would be tempted to associate the dusk enhancements with either the classical plasmapause boundary or with detached regions of the plasmasphere. This idea is certainly supported by comparison of figure 5c with 5d, and by the fact that these low-energy events occur predominantly when the geomagnetic disturbance index, Kp, is low. Although it is generally believed that the plasmasphere is populated by very low-energy (~ 0.1 eV) ionospheric plasma, there is no *a priori* reason to believe that the original cold plasma could not be heated by a process such as ring-current interactions or acceleration by electric fields parallel to the magnetic field. The distribution in local time and relation to Kp suggest a plasmaspheric origin for at least some of these events, and the observations suggest that indeed the outer regions of the plasmasphere are considerably warmer than has previously been supposed.

(a)

ION DUSK ENHANCEMENT

AUG. 20, 1974
0036 UT
PITCH ANGLE ~23°

~ZERO
COUNT RATE

(b)

DUSK REGION ENHANCEMENT

AUGUST 20, 1974
0030-0050 UT
~30 eV

ELECTRONS

IONS

(c)

WARM PLASMA EVENTS
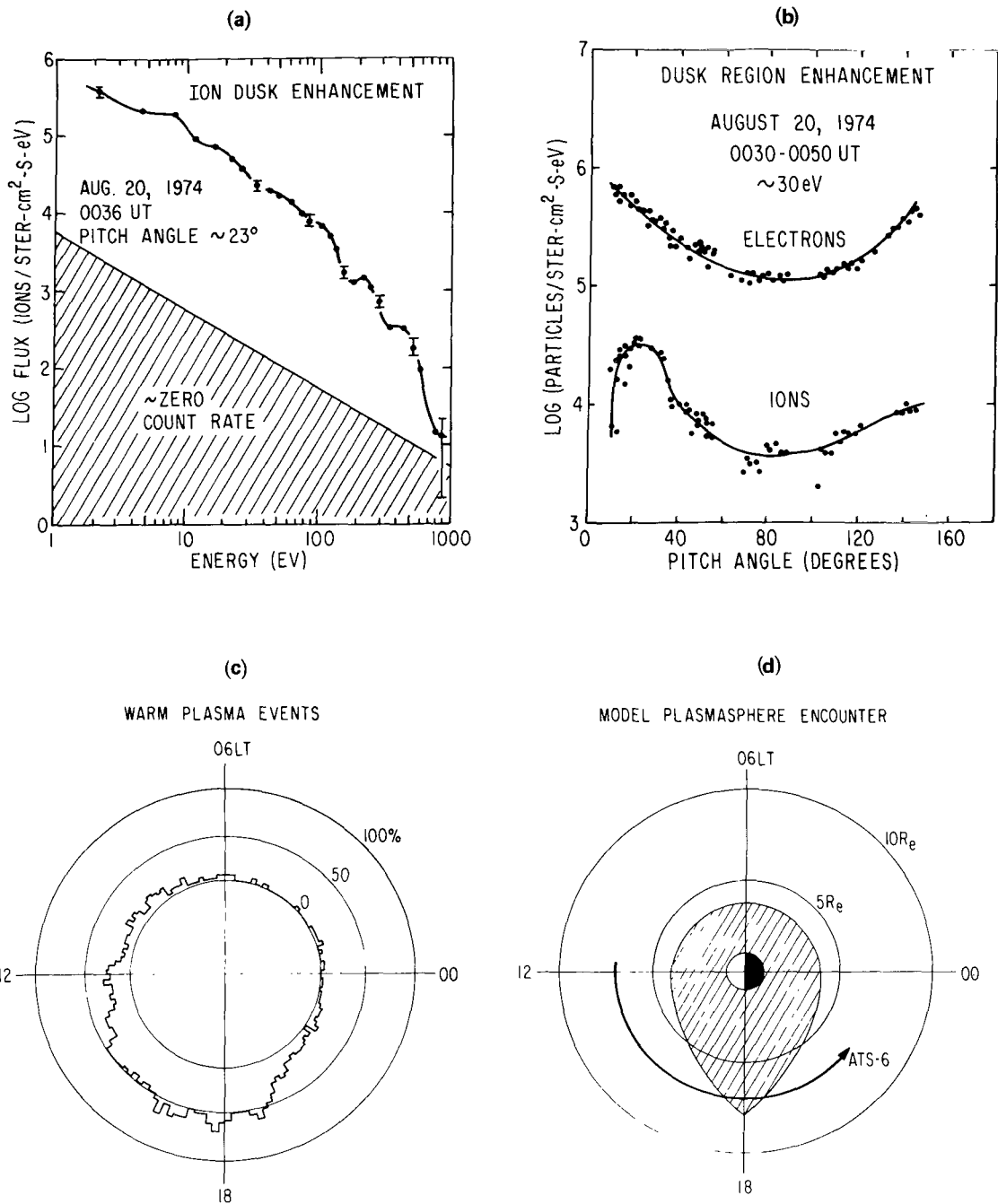
(d)

MODEL PLASMASPHERE ENCOUNTER

Figure 5. Dusk region low-energy enhancement. Quadrant a) shows a quasi-Maxwellian ion distribution with a temperature between 5 and 20 eV recorded at 1836 LT at the peak of the pitch-angle distribution shown in quadrant b). Quadrant c) shows the local time distribution of percentage encounters by ATS-6 with the low energy, low temperature (2 to 30 eV with densities of 1 to 10 ions/cm^3) ions. Quadrant d) shows a model plasmasphere encounter by ATS-6 which can be compared with quadrant c). All data were taken by the UCSD electrostatic analyzers.

CORRELATED PERIODIC VARIATIONS OF PARTICLES AND THE MAGNETIC FIELD

An unusually large number of correlated wave and particle oscillations have been observed by the ATS-6 EME instruments while the satellite was located at 94°W longitude. The number of events appears to be matched only by the variety in the wave and particle characteristics. This surprising variety of observations may be a function of the satellite's location 10° off the magnetic equator or the result of an extremely low noise magnetometer and well-designed and functioning particle instruments or a combination of both factors.

Wave and Particle Observations of Pc 1 Oscillations

ATS-6 has, for the first time, observed Pc 1 oscillations simultaneously in magnetic and particle data in the equatorial magnetosphere. The lower portion of figure 6 shows 5-second oscillations in the energy flux of two UCSD ion detectors (set at 30 eV). The look directions of the two detectors are antiparallel when projected onto a plane perpendicular to the local magnetic field. Note that the oscillations in the figure observed in the responses of these two detectors are 180° out of phase. By using these two detectors in conjunction with a third not represented in the figure, the bulk velocity vector associated with these oscillations is observed to gyrate in a left-handed elliptically polarized sense. The insert to figure 6 shows a magnetic hodogram during several cycles of the particle oscillations. The magnetic field data have been transformed to a field-aligned coordinate system with the z-axis parallel to B and the x-axis eastward.

The perturbation magnetic vector also gyrates in the sense of left-handed polarization. The double arrows in the inserted figure are positioned at those points in time when one of the three ion detectors displays a peak in its count rate. The bulk velocity direction at that point in time is antiparallel to the detector look direction and is represented by an "open" arrow in the figure. The perturbation magnetic vector ("closed" arrow) is obtained by drawing an arrow pointing away from the center of the appropriate ellipse of the hodogram. From the figure it is clear that the perturbation flow velocity is antiparallel to the perturbation magnetic field. These oscillations are likely to be traveling left-handed polarized Alfven waves. This Pc 1 event occurred during a large amplitude Pc 4 event discussed later in the section, "Ring Current Proton ULF Waves."

The Pc 1 oscillations have been observed predominantly within the dusk region low-energy enhancements discussed in the section, "The Unexpected Existence of a Warm Plasma in the Region of the Plasmaspheric Bulge," with periods anywhere from 1 to 10 s (the proton gyroperiod in this region is about 0.6 s). Also, the particle perturbations are observed predominantly within the low-energy detector channels ($\lesssim 50$ eV), because the flow velocity associated with the waves (5 to 50 km/s) is a small perturbation on the particle velocities at higher energies.
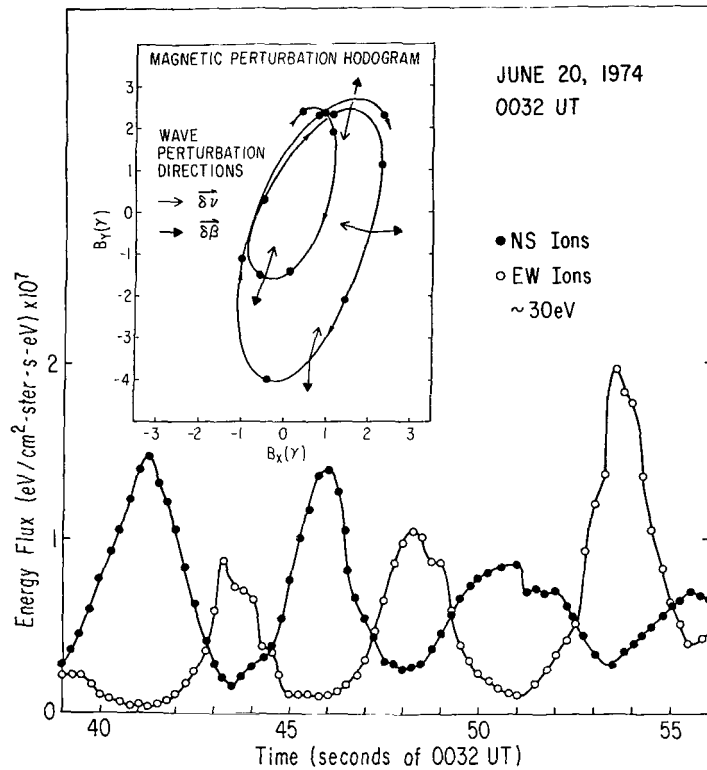
Figure 6. Alfven wave observations. The lower portion shows the energy flux of 2 of 3 UCSD ion detectors (set at 30 eV). When the detector look directions are projected onto a plane perpendicular to the local magnetic field, the projected vectors look nominally antiparallel. The insert shows a hodogram using UCLA data where B_x points eastward. The double arrows show that the perturbation magnetic field and bulk velocity vector point nominally antiparallel.

Particle and Field Measurements of Standing ULF Waves

Oscillating plasma flows and associated ULF magnetic oscillations have been observed with the UCSD particle experiment and the UCLA magnetometer experiment. On June 27, 1974, a Pc 4 event occurred that had a peak magnetic amplitude of 10γ and a period of 150 seconds. The transverse magnetic wave was linearly polarized in the east-west (azimuthal) direction. During a large segment of the event, the three UCSD ion detectors lay in a plane, with two of the detectors viewing in opposite directions along the east-west axis and the third viewing perpendicular to this axis in the radial direction. From the response of these three detectors, it is possible to construct the particle-distribution function in this plane and to determine its first moment, the flow velocity (v). In this plane, the flow velocity was also linearly polarized, primarily in the east-west direction, and had a peak amplitude of 140 km/s. By constructing the vector cross product of v with the static

magnetic field, it is possible to infer the electric field, E_v. Having both the E and B components of the wave, Poynting's vector, S_k, can be constructed in order to determine the propagation characteristics of the wave. Note that the flow component parallel to B is not necessary for this calculation. These factors are displayed in figure 7. The magnetic and electric components of the wave are out of phase by 90°, and the value of S_k oscillates around a value of zero. The relative phase of the wave components and the behavior of S_k are consistent with an interpretation of the event as the occurrence of the fundamental mode of a standing hydromagnetic wave on the ATS-6 field line; that is, there is no net flow energy.
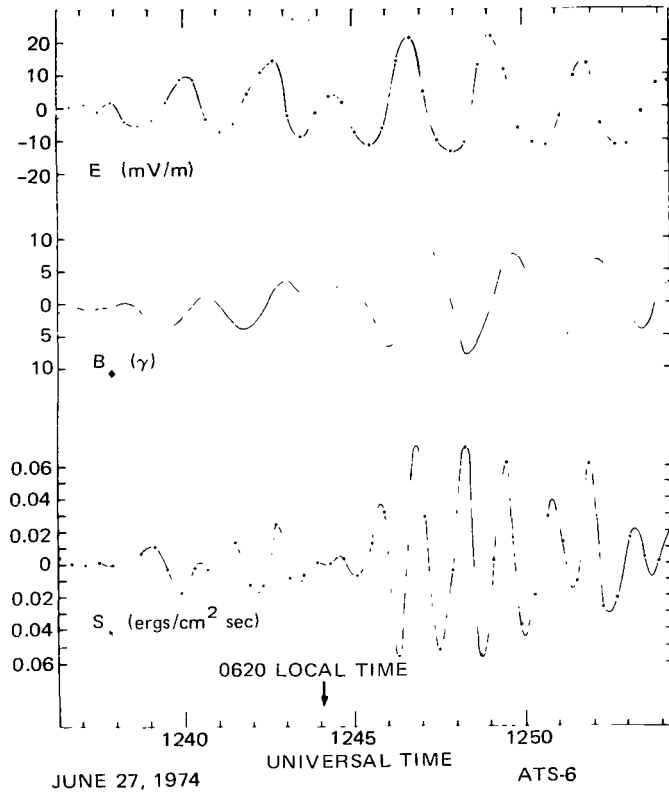

Figure 7. Determination of Poynting's vector as a function of time, using the electric field perpendicular to B inferred from particle-flow measurement and the measured magnetic field.

Cummings et al. (Reference 10) have presented a model concerning standing hydromagnetic or Alfven waves. Extending this model and using the time dependence of the Bϕ component presented in figure 7, it is possible to theoretically predict the magnitude and time variation of the flow velocity. The theoretical and measured values of v agree on the average to within ±17 km/s, which is about 25 percent of the average amplitude of the velocity wave.

11

Ring Current Proton ULF Waves

Seventy-one cases of ultralow frequency oscillations of proton-flux intensities were detected by the National Oceanic and Atmospheric Administration (NOAA) instruments from June 11 to September 16, 1974. The oscillation periods ranged from 40 seconds to 6 minutes, which correspond to Pc 4 and Pc 5 in magnetic pulsation terminology. Most of the waves were observed in the dusk region of the magnetosphere. Figure 8 presents an example of such a wave event compiled from data recorded by the NOAA and UCLA experiments on June 20, 1974, when ATS-6 was in the dusk magnetosphere. In the upper panel of the figure, the proton flux intensities detected by the NOAA proton detector telescope C are shown. It is seen that the proton flux intensities exhibit an almost sinusoidal oscillation with a period of ~126 seconds in four energy channels from E = 48 keV to E = 234 keV. The fluxes in the two lowest energy channels show little oscillation. The largest ratio of j_{max} to j_{min} during any single cycle of oscillation was observed to be as large as 2.5. Although the wave had a larger persistent amplitude in the 4th ($71 \leqslant \Delta E \leqslant 100$ keV) and the 5th ($100 \leqslant \Delta E \leqslant 151$ keV) energy channels, the largest amplitude of the wave was detected in the 6th ($151 \leqslant \Delta E \leqslant 234$ keV) energy channel at ~0030 UT. It should be emphasized that the flux oscillations presented here are not caused by the so-called intensity modulation corresponding to the changes in the proton pitch angles detected by telescope C. The proton pitch angles shown in the middle panel of the figure indicate no systematic correlation with the flux intensities.

In the bottom panel of figure 8, UCLA fluxgate magnetometer data have been plotted in the dipole VDH coordinates described in the section, "Inclination of the Magnetic Field at ATS-6." There are two distinct wave phenomena simultaneously present, Pc 4 with a period of 126 seconds and Pc 1 with a period of 5 seconds. Only the low frequent wave correlates with the energetic proton oscillations shown in the top half of the figure. As noted in the section, "Wave and Particle Observations of Pc 1 Oscillations," however, the high frequency Pc 1 wave is well correlated with lower energy protons seen by the UCSD detector.

The low frequency Pc 4 wave had a maximum amplitude of approximately 10γ, primarily in the V-component. Spectral analysis shows that the signal was linearly polarized, radially inward in the meridian plane. Since the ambient field was tilted inward, the wave had a substantial compressional component as evident in the oscillations of the field magnitude. Examination of the V-component data between 0029 and 0040 UT suggests that the Pc 4 wave is modulating the amplitude of the Pc 1 wave. We note however, that the Pc 1 amplitude maxima occur at minima of the total field; that is, during the rarefaction phase of each cycle. It seems likely, therefore, that the Pc 4 wave is not stimulating Pc 1 wave growth via compression of the proton pitch-angle distribution and ion-cyclotron instability. Instead, it is more likely that unstable plasma is being swept back and forth across the spacecraft by the electric field associated with the Pc 4 wave.

The field and particle correlation is not obvious at first glance in figure 8 due to the fact that the proton fluxes have a phase shift as a function of energy. The highest energy channel protons peak first in intensity during each cycle of oscillation. The peak flux intensities
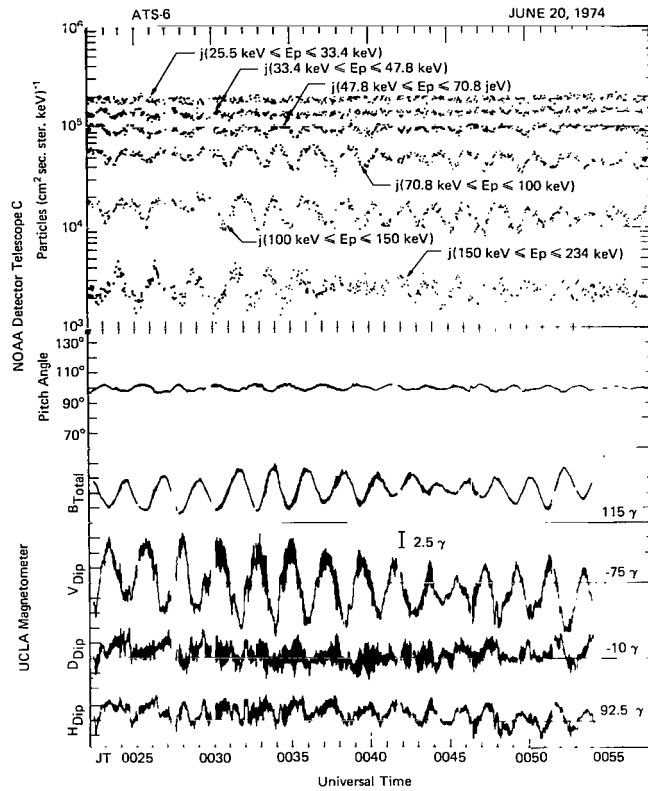
Figure 8. Observations of Pc 4 frequency oscillations in energetic protons and magnetic field. The period of the oscillations is ~126 seconds.

are then detected in progressively lower energy channels. Such energy-dependent dispersion in the phase of the flux oscillations is very similar to the energy-dependent dispersion in the arrival of drifting proton clouds. The observed phase difference cannot be due to the different drift velocities of the observed protons. In the case of drifting proton clouds, the time delay between the peaks in the two adjacent lower energy channels would be longer than that between the peaks in the two adjacent higher energy channels if the drifting plasma were injected within a finite region of the magnetosphere. The observed time difference between the peak fluxes for each pair of adjacent energy channels is shorter for the lower energy channels than for the higher energy ones. Su, Konradi, and Fritz (Reference 11) have concluded that the phase difference was caused by the finite gyroradius effect of the protons associated with waves in a nonuniform magnetic field. When such an effect on the first-order perturbed particle distribution function is examined, it is possible to determine that the wave propagated in a westward direction around the Earth with a phase velocity of 13.4 (±9.6) km/s. This wave also had a radial phase velocity of 0.15 (±0.09) km/s propagating inward toward the Earth. When the phase factor of the proton flux oscillations has been taken into account, one finds that the particles and the field oscillated 180° out of phase.

13

Energetic Electron Waves at Synchronous Orbit

Approximately 25 cases of well-defined low frequency oscillations of electron fluxes have been observed by the McDonnell-Douglas Astronautics Company (MDAC) electron spectrometer during the first 3 months of observation. The experiment is capable of 0.25-s time resolution. However, the routine survey plots utilized in this preliminary data analysis contain 30-s averages, and thus oscillations having periods shorter than ~3 minutes cannot be observed. The oscillations observed to date show no local time preference. Two types of oscillations have been observed: the first is characterized by phase differences between the various energy channels indicating energy-dependent dispersion of the electron waves. The second type of oscillation observed is characterized by complete phase correlation between all of the electron channels. Figure 9 shows one of these wave events as observed by the MDAC electron spectrometer and the UCLA magnetometer when ATS-6 was near the dusk meridian. The 50- to 100-keV perpendicular ($E_{1\perp}$) and parallel ($E_{1\parallel}$) and the 200- to 400-keV perpendicular ($E_{3\perp}$) and parallel ($E_{3\parallel}$) electron channels are shown, as well as the UCLA magnetometer data. The electron oscillations are in phase and larger for the higher energies. (The 400- to 1000-keV amplitudes, which are not shown, are the same as the 200- to 400-keV amplitudes.) There is, however, no generalization that can be made between oscillation amplitudes and energy. There exist as many cases having a maximum oscillation at low energy (50 to 100 keV), as ones having a maximum at high energy (400 to 1000 keV). The UCLA magnetometer data plotted in the VDH dipole coordinate system are characterized by high frequency Pc1 waves modulated by the longer period Pc 4 waves. The electron oscillations are 180° out of phase with the magnetometer oscillations.

Large-Scale Trapping Boundary Waves

Large rapid decreases in the energetic proton flux followed by even more rapid increases are characteristic of disturbed periods on ATS-6 (References 12 and 13). In order to unambiguously interpret such observations made on a moving spacecraft, it is necessary to be able to separate spatial from temporal variations. One approach to this problem is to use proton flux gradient information, since, if a flux change is accompanied by a change in the gradient, the motion of a system over the spacecraft may be inferred. The energetic proton experiments on ATS-6 are uniquely suited to determine the proton flux gradient. The University of Minnesota experiment contains two nearly identical detector assemblies, which, when directed oppositely, can examine the flux of protons orbiting about gyrocenters displaced by up to two Larmor radii from one another. Thus, the spatial flux gradient along a line between the gyrocenters can be computed. The NOAA experiment contains three detector systems directed such that the gyrocenters of protons entering these detectors lie on a line orthogonal to the line through the gyrocenters of protons entering the Minnesota experiment. As the instruments respond to overlapping energy ranges, it is possible to determine the flux gradient at a given energy using data from these two experiments.
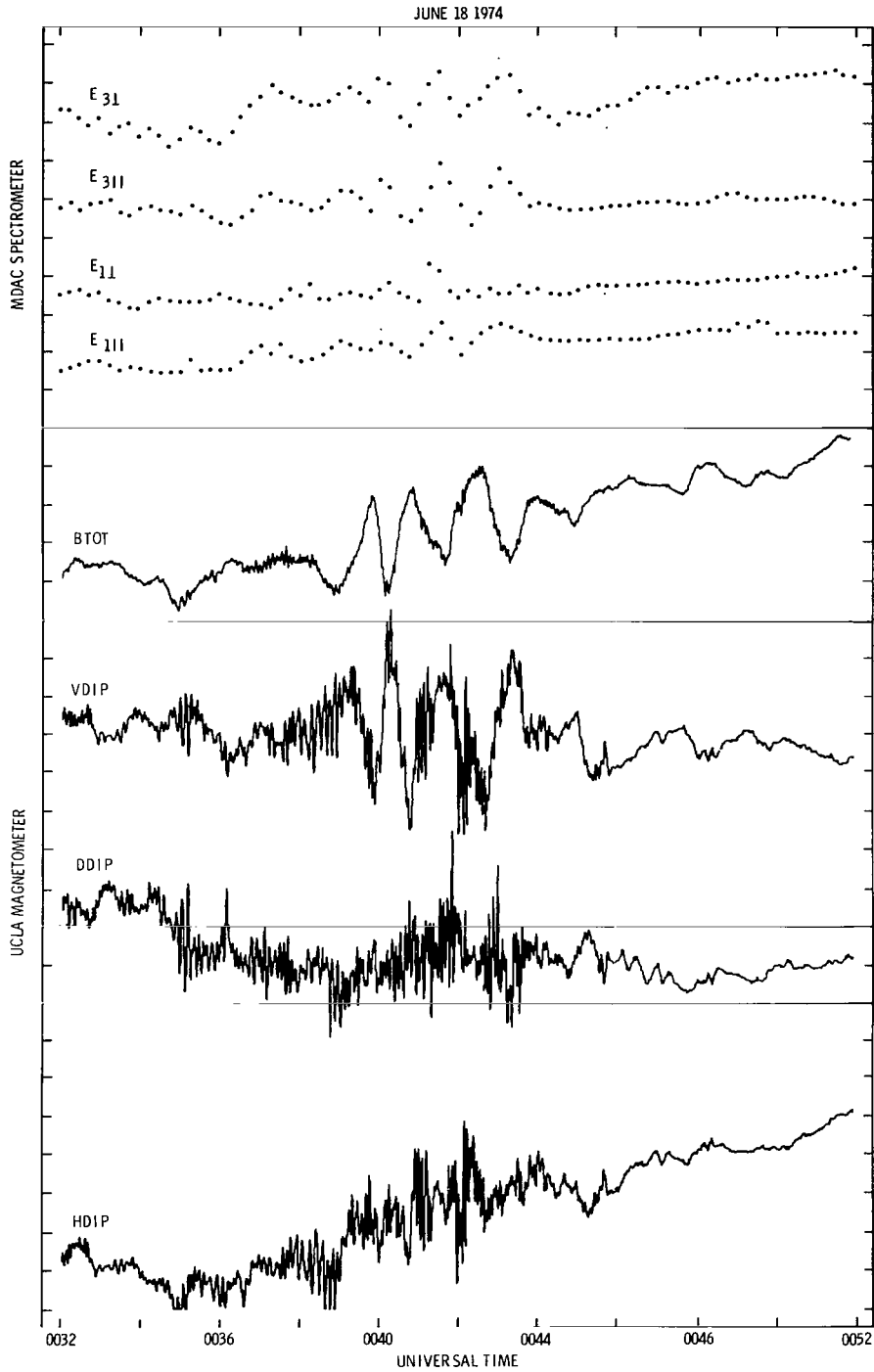
Figure 9. Low frequency electron flux oscillations. In the upper panel, MDAC electron channels E_1 (50 to 100 keV) and E_3 (200 to 400 keV) are presented for nominal perpendicular ($\perp$) and parallel ($\parallel$) configuration to the local field. The lower panel contains the UCLA magnetometer data.

15

The use of this technique is demonstrated in figure 10. Here, a brief section of the data from July 5, 1974 is presented. These observations were made when ATS-6 was at approximately 0800 local time during a magnetic storm. During the July 4 through 6 storm period, the particle experiments recorded a total of 23 rapid decreases and recoveries such as the one presented in figure 10 (Reference 12). The top two curves show 3-s averages of the flux of 60-keV protons from the two Minnesota detectors, while the lower curves give the 60-keV flux from the B and C telescopes of the NOAA experiment. Since the energy channels of the two instruments differ, the flux values were determined by using a least-squares fit on the measured energy spectra from each detector, and determining the flux at 60 keV from the fit. The dashed sections in the curves are drawn through data gaps. The location of the gyrocenters of protons entering the detectors are plotted in dipole VDH coordinates (see the section, "The Inclination of the Magnetic Field at ATS-6") in the insert. The gyro-centers of protons entering the Minnesota scanning detector were north and tailward of ATS-6, and those entering the east-looking detector were south and Earthward. The protons entering the NOAA B detector were west of the ATS-6, while those entering the C detector were east of the satellite. These locations were calculated for the particle recovery and only give approximate positions for the remainder of the event.
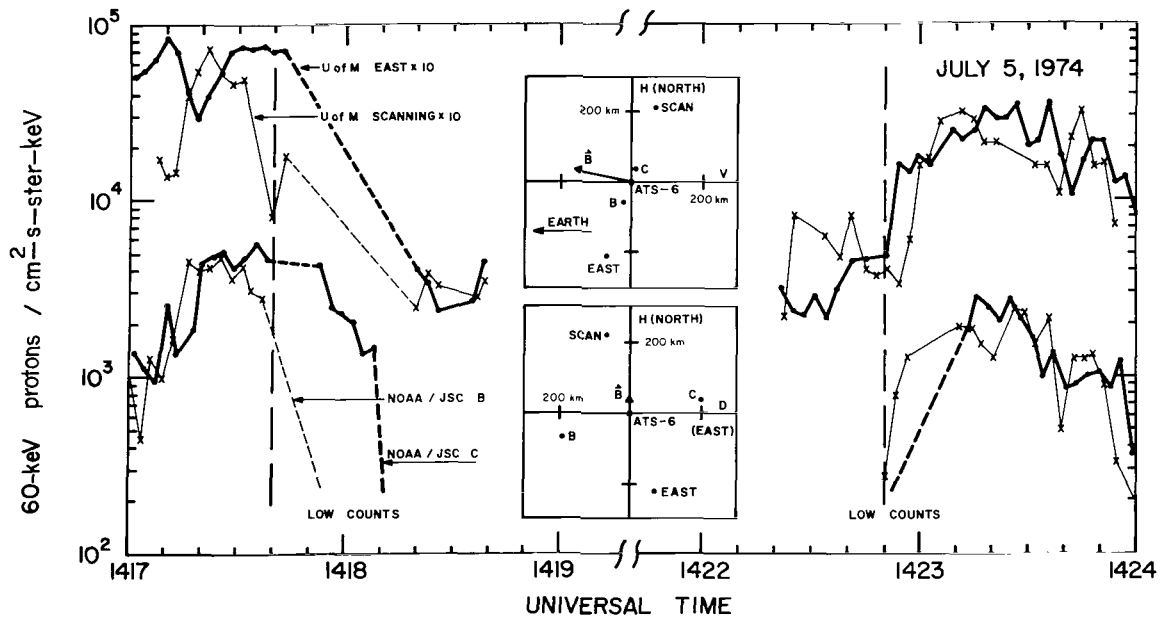

Figure 10. Sixty-keV proton fluxes from the University of Minnesota (U of M) experiment (top) and the NOAA experiment (bottom). The center insert shows the location of the gyrocenters of protons entering the four detectors in Dipole VDH coordinates.

The decrease represents motion directed toward the south and east of ATS-6 but the velocity corresponding to this motion cannot be calculated unambiguously.

The interpretation of the subsequent increase is much clearer. The increase occurs simultaneously in the data from the Minnesota east detector and that from the NOAA B spectrometer. The increase starts approximately 5 seconds later in the scanning detector and the C detector. Thus, these increases represent the motion of a boundary approaching from the south and west of ATS-6, and moving toward the northeast with a velocity of about 58 km/s. The large eastward component of the velocity (41 km/s) and the repeatability of this variation in the flux gradients has led Su, Fritz, and Konradi (Reference 12) to interpret this as a large-scale wave traveling eastward around the Earth.

Other proton flux decreases and recoveries observed during magnetospheric substorms are confined to the nightside magnetosphere. All of the decreases are consistent with the motion of the trapped particle region Equatorward and Earthward of the satellite. The motion corresponding to these flux increases may be organized into three types according to the direction of the gradient. Some particle increases have been interpreted as motion from Earthward and Equatorward of ATS-6. The majority of the recoveries represent motion presumably of the plasma sheet from north and tailward of the spacecraft. In the premidnight region, a recovery from beneath the satellite is followed by motion from north and tailward of ATS-6 (Reference 13).

Modulation of Energetic Electrons in Association with the Sector Boundaries of the Interplanetary Magnetic Field

The Aerospace Corporation energetic-particle spectrometer aboard ATS-6 has observed a periodicity in the energetic electron fluxes ($E_e > 1$ MeV) associated with the passage of sector boundaries of the interplanetary magnetic field (IMF). The changes in the electron flux associated with each boundary passage are the major variability in the electron fluxes during conditions of low solar activity.

Data obtained during the fall of 1974 are presented in figure 11 along with the sector boundaries of the IMF obtained from the catalog prepared by Svalgaard (Reference 14). The ATS-6 electron fluxes (hourly averages) exhibit a very pronounced periodicity that is very clearly associated with the passage of interplanetary magnetic-field sector boundaries. Figure 11 illustrates the observations made at local noon. Similar plots have been constructed for other local times, and these plots exhibit identical periodicities. A limited set of data from ATS-1 and ATS-5 is also available for the same time period. Such comparisons indicate that ATS-1, ATS-5, and ATS-6 all observe the modulation just described; that is, the modulation is clearly one which affects the entire magnetosphere.

A similar study was conducted using ATS-1 data from the Aerospace Corporation spectrometer taken in 1967 and 1968, the period near solar maximum. In that study, it was not possible to establish that any close correlation existed between changes in the electron fluxes observed at synchronous altitude and changes in the direction of the interplanetary field.
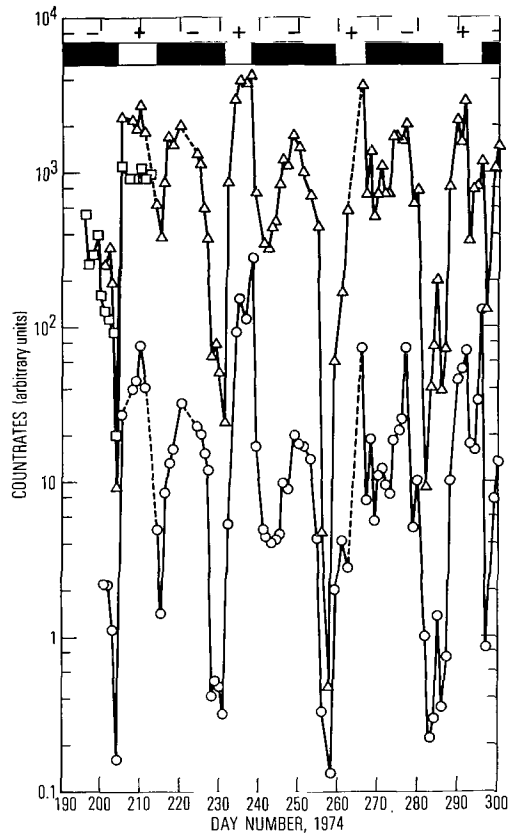
Figure 11. Hourly averages of energetic electron count rates observed by ATS-6 and ATS-1 are plotted as a function of Day Number, 1974. Also plotted (at the top of the figure) is the polarity of the interplanetary magnetic field as inferred by Svalgaard (Reference 14). Local time for all particle data is local noon; the sector boundary transitions are assumed to occur at 0000 UT for the days indicated. Circles and triangles are ATS-6 observations of > 3.9- and > 1.6-MeV electrons, respectively, and squares are ATS-1 observations of > 1.9-MeV electrons.

To be sure, sector boundary passages did give rise to major excursions in the flux levels of energetic electrons; however, equally large excursions also occurred when there were no IMF boundaries in the vicinity of the Earth. Apparently, during periods of high solar activity, the sector structure modulation is masked by the more-or-less irregular occurrence of magnetic storms that destroy the coherence exhibited by the energetic electron fluxes during quiet time.

18

The energetic electrons of the outer radiation belt observed by ATS-6 are one of the end-products of the interaction of the solar wind with the Earth's magnetosphere. The magnetospheric substorm is the basic process which both energizes the magnetospheric plasma and transports this heated plasma within the magnetosphere. Observing the energetic electron population thus amounts to observing the averaged, smoothed output of the solar-wind magnetosphere engine. Studies of the temporal evolution of energetic electron fluxes on time scales of days can give some interesting insight into the overall coupling between the solar wind and the magnetosphere. The energy flow from the solar wind into the magnetosphere in some ways mimics the behavior of a half-wave rectifier, familiar in electronic applications. The input of energy into the magnetosphere proceeds only if the magnetosphere sees a southward component of the interplanetary magnetic field; a northward IMF component apparently inhibits the transfer of energy into the magnetosphere (see a review by Russell (Reference 15) and the references therein). Thus, to a first approximation, magnetospheric dynamics are a function of the orientation of the magnetosphere in solar-equatorial coordinates (the natural coordinates of interplanetary plasma flow). The geometrical arguments, taken together with the complexity of the interplanetary field structure, result in a fairly complex picture of the interaction between solar wind and magnetosphere that can be summarized briefly in the following manner: the interaction between the solar wind and the magnetosphere is strongest in the spring for inward (-) directed interplanetary sectors and strongest in the fall for outward (+) interplanetary sectors. Our findings are in agreement with this suggestion. In figure 11 (containing data obtained during the fall of 1974) the energetic electron fluxes appear to build up to higher levels during (+) sectors than during (-) sectors. A limited set of data obtained in early 1975 appears to indicate that in spring, (-) sectors result in higher fluxes of energetic electrons.

THE EXISTENCE OF DOMINANT FLUXES OF ENERGETIC HEAVY IONS

The NOAA heavy-ion instrument has provided the first definitive measurements of energetic heavy ions present in the vicinity of the geostationary orbit. The detector system is a two-element solid-state detector telescope which incorporates an extremely thin (3.8-micron) front element in order to accomplish ion nuclear charge (Z) identification by a dE/dx and E technique. In a single reasonably isolated injection event which occurred at ~0030 UT on June 18, 1974, the presence of ions with $Z \geqslant 6$ and $E > 4.0$ MeV in the vicinity of the geostationary orbit was established. By noting that similar detectors carried on board the Interplanetary Monitoring Platform (IMP) H and J satellites were responding at background levels in the interplanetary medium for 4 days surrounding this event, it was concluded that these ions are energized within the magnetosphere during these substorm-type events.

In figure 12, the differential energy spectra constructed for the event period are presented. Note that the intensity of these ions dominates the intensity of protons at the same energy above 0.5 MeV. These ions are most probably oxygen. This result indicates that care should be exercised in identifying any response of a nondiscriminating ion detector as a "proton" response. If such a detector discriminates only on energy (as do most lower energy
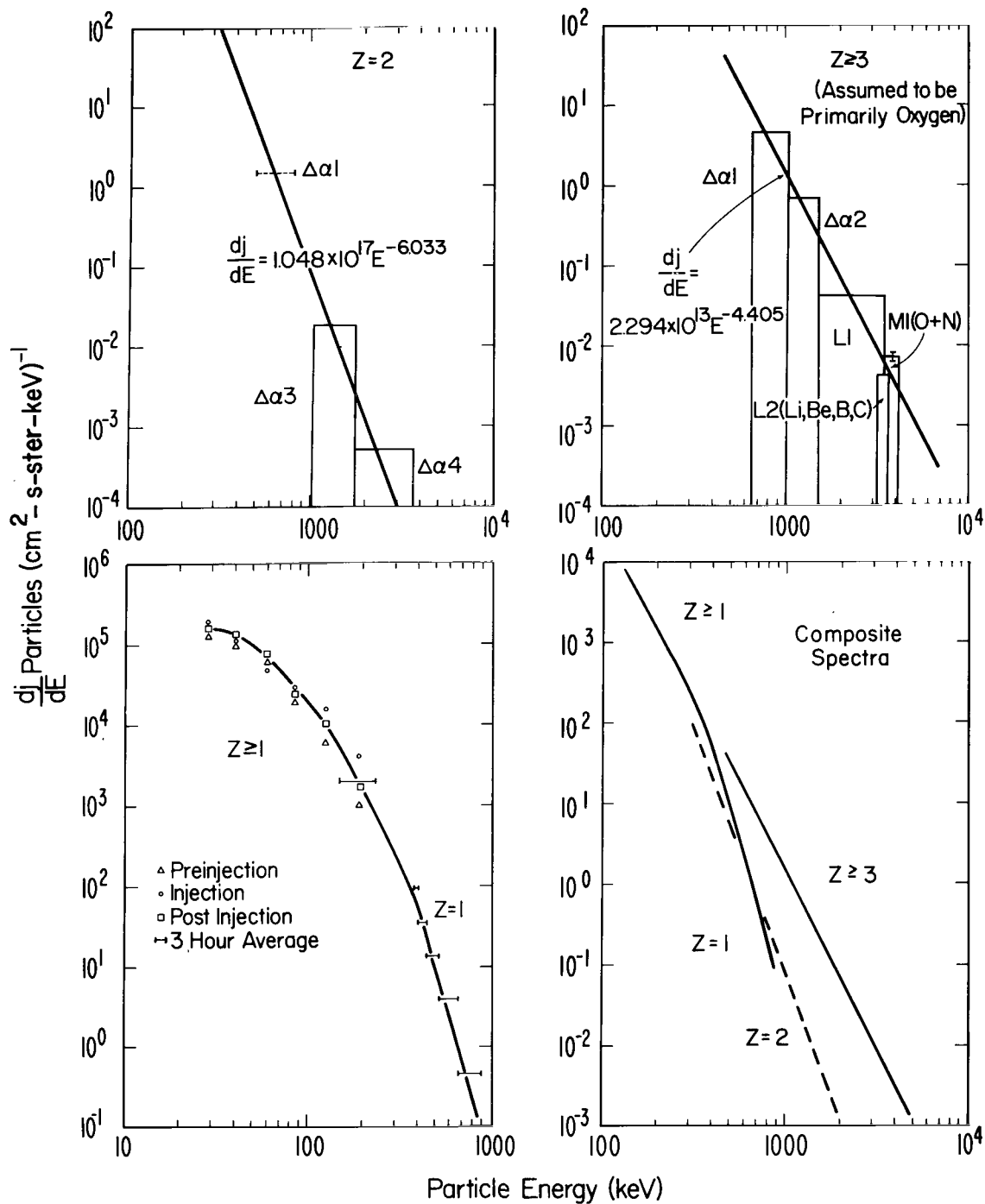
Figure 12. The differential energy spectra for ion species identified by the NOAA instrument constructed from an average of all responses over the time period 00 to 03 UT on June 18, 1974.

solid-state detectors flown to date), ions heavier than protons can easily dominate its response at these energies (Reference 16).

TYPICAL PARTICLE SPECTRA

It is difficult to locate in the literature particle-energy spectra measured instantaneously in the magnetosphere that cover more than a limited energy range or display more than one particle species. The EME particle instruments are capable of performing measurements on both the electron and ion differential intensities over an energy range from less than 1 electron volt to greater than 100 million electron volts. In figure 13, simultaneously measured differential energy spectra covering twelve orders of magnitude in flux are presented for locally mirroring electrons and ions that were observed on July 20, 1974.

SPACECRAFT CHARGING EFFECTS

Spacecraft in the vicinity of the geostationary orbit have been shown to charge to various potentials that depend on conditions in the local plasma environment of the satellite (Reference 17). A more detailed picture of spacecraft charging effects is beginning to emerge from the ATS-6 data than was available before. A peak in the counting rate of the low-energy (4 to 10 eV) electron detectors of the UCSD experiment has been shown to be due to photoelectrons and/or secondary electrons which have been emitted by the spacecraft and are returning to it (Reference 18). This implies the presence of a potential barrier about the spacecraft. However, the barrier, which keeps out low-energy plasma electrons as well, is too large to be explained in terms of a simple space-charge effect (Reference 19). It now appears that the satellite is differentially charged, with parts of the spacecraft, such as the solar arrays, at a more negative potential than the main spacecraft body. The resulting electric-field pattern is responsible for the potential barrier effect, as illustrated in figure 14. ATS-6 has been observed to charge to a potential of -2200 volts during sunlit conditions and to a potential of -19,000 volts during eclipse periods.

SUMMARY

These initial results from ATS-6 demonstrate the existence of two new particle populations, even though, after nearly two decades of magnetospheric exploration, many researchers feel that all the significant particle populations of the magnetosphere have been identified and their morphological features well-documented. The unexpected existence of a warm plasma in the vicinity of the plasmaspheric bulge and the existence of dominant fluxes of energetic ions heavier than protons produced during substorms must now be incorporated into presently held concepts of the magnetosphere.

The initial results from the EME instruments on ATS-6 have provided significant insight into the role of currents in the magnetosphere and the probable carriers of these currents, particularly in the case of field-aligned substorm-associated currents whose particle signature has been observed for the first time near the equatorial plane.
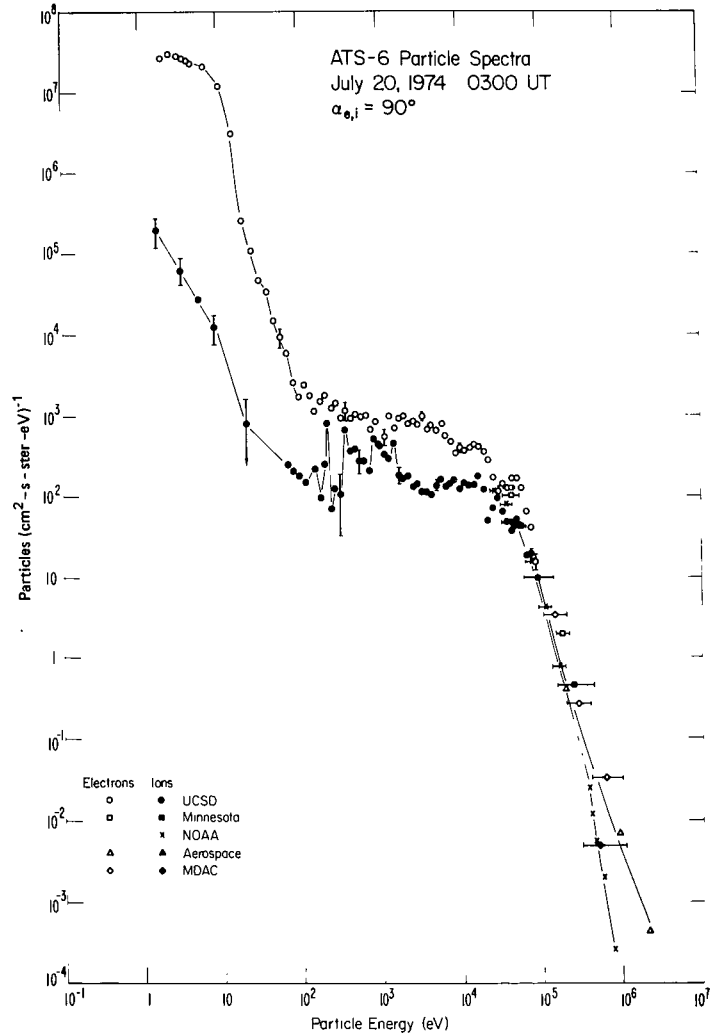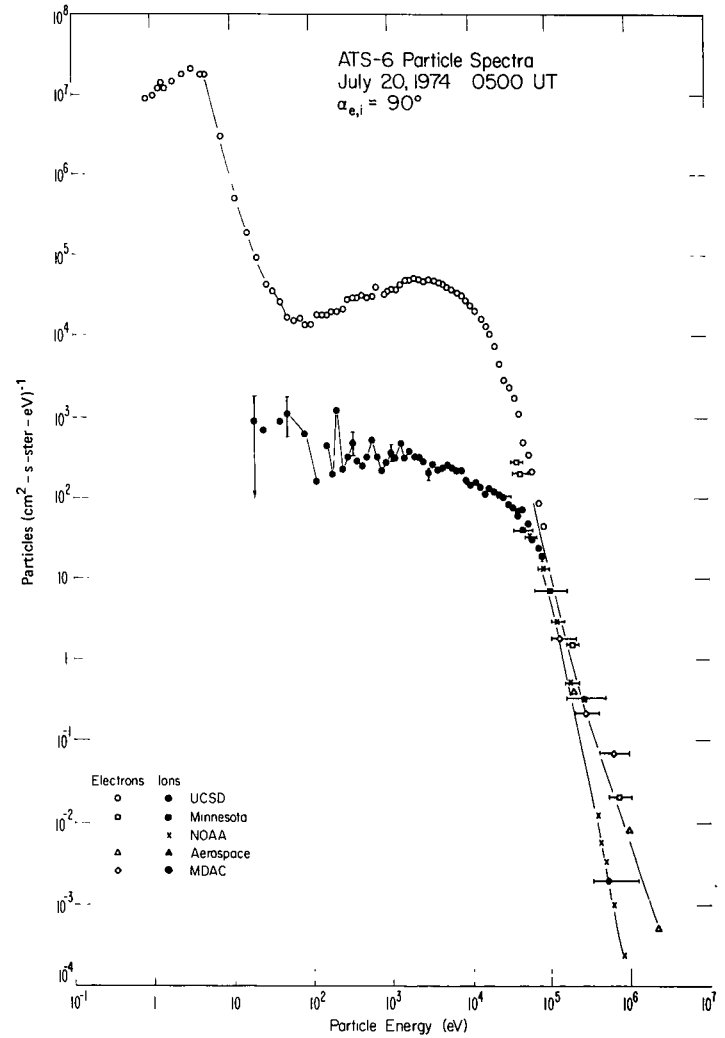
Figure 13. Instantaneous energy spectra for electrons and ions measured for locally mirroring particles at ATS-6. These spectra cover eight orders of magnitude in energy and twelve orders of magnitude in particle flux.
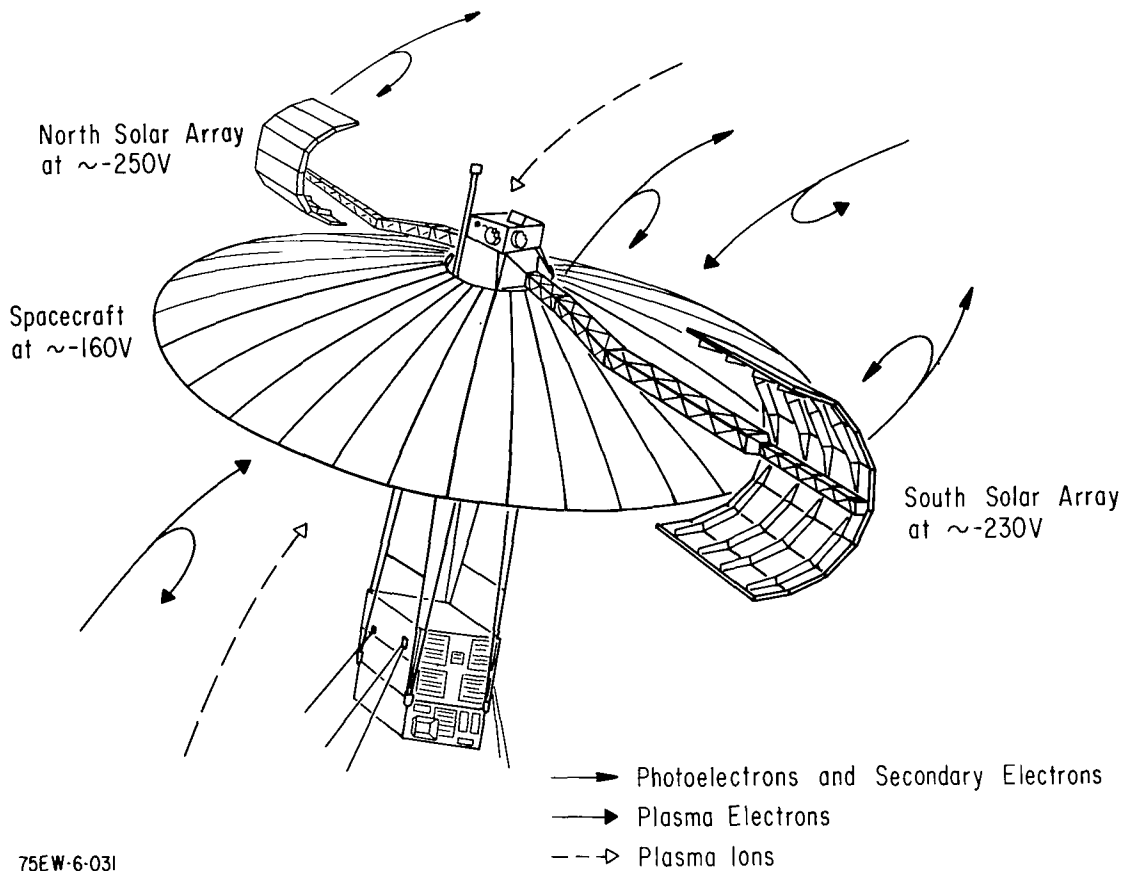
North Solar Array at ~-250V

Spacecraft at ~-160V

South Solar Array at ~-230V

⟶► Photoelectrons and Secondary Electrons

⟶► Plasma Electrons

— —▷ Plasma Ions

75EW-6-031

Figure 14. On day 248 (September 5, 1974) it could be inferred from the UCSD ion detectors that the spacecraft potential was about -160 V (at 0855 UT). In addition to the plasma electrons and the low-energy photoelectrons from the spacecraft, the electron detectors which looked in the north-south plane also saw a sharp spike at an energy which depended upon the look-angle. The spike is believed to be due to electrons emitted from the solar arrays which are at a more negative potential than the rest of the spacecraft.

The large variety of wave and particle interactions observed on ATS-6 will prove invaluable in delineating many of the specific acceleration and transport mechanisms active on the hot-plasma distribution in the region of the geosynchronous magnetosphere. The fact that such a large variety of interactions has been observed indicates that there are probably many mechanisms at work simultaneously in any one substorm or combination of substorm events.

The results presented in this document mark the beginning of what promises to be a very successful satellite program. As further studies are undertaken involving correlations between the various EME instruments themselves, with other satellites, and with ground-based programs, even more significant results should be forthcoming.

ACKNOWLEDGMENTS

The authors would like to express their appreciation to the ATS Project Office at NASA/ GSFC and the support of Mr. R. O. Wales and Mr. F. H. Wainscott. The EME program support provided by the NASA Office of Space Sciences, Physics and Astronomy Directorate (Code ST) is also gratefully acknowledged.

24

REFERENCES

1. McPherron, R. L., P. J. Coleman, and R. C. Snare, "ATS-6 UCLA Fluxgate Magnetometer," *IEEE Trans: Aerospace and Electronic Systems*, AES-11(6), 1975, pp. 1110-1117.

2. McIlwain, C. E., "Auroral Electron Beams Near the Magnetic Equator," in *Nobel Symposium 30th: Physics of the Hot Plasma of the Magnetosphere*, B. Hultqvist and L. Stenflo, eds., Plenum Press, N. Y., 1975, pp. 91-112.

3. Mead, G. D., "Deformation of the Geomagnetic Field by the Solar Wind," *J. Geophys. Res.* 69, 1964, pp. 1181-1194.

4. Pfitzer, K. A., *The Expected Quiet Time Magnetic Field at ATS-6*, McDonnell-Douglas Corp. Space Sciences Dept., August, 1974.

5. Olson, W. P., and K. A. Pfitzer, "A Quantitative Model of the Magnetospheric Magnetic Field," *J. Geophys. Res.*, 79, 1974, pp. 3739-3748.

6. Anderson, H. R., and R. R. Vondrak, "Observations of Birkeland Currents at Auroral Latitudes," *Rev. Geophys. and Space Phys.*, 13(1), 1975, pp. 243-262.

7. Sugiura, M., "Identifications of the Polar Cap Boundary and the Auroral Belt in the High-Altitude Magnetosphere: A Model for Field-Aligned Currents," *J. Geophys. Res.*, 80(16), 1975, pp. 2057-2068.

8. Coleman, P. J., Jr., and R. L. McPherron, "Fluctuations in the Distant Geomagnetic Field During Substorms: ATS-1," in *Particles and Fields in the Magnetosphere*, B. M. McCormac, ed., Advanced Study Institute, Earth's Particles and Fields, University of California, Santa Barbara, 1969, pp. 171-194.

9. McPherron, R. L., C. T. Russell, and M. P. Aubry, "Satellite Studies of Magnetospheric Substorms on August 15, 1968. Part 9. Phenomenological Model for Substorms," *J. Geophys. Res.*, 78(16), 1973, pp. 3131-3149.

10. Cummings, W. D., R. J. O'Sullivan, and P. J. Coleman, Jr., "Standing Alfven Waves in the Magnetosphere," *J. Geophys. Res.*, 74(3), 1969, pp. 778-793.

11. Su, S. Y., A. Konradi, T. A. Fritz, "On the Propagation Direction of Ring-Current Proton ULF Waves Observed by ATS-6 at 6.6 R_E," *J. Geophys. Res.*, 82, 1977, pp. 1859-1868.

12. Su, Shin-Yi, T. A. Fritz, and A. Konradi, "Repeated Sharp Flux Dropouts Observed at 6.6 R_E During a Geomagnetic Storm," *J. Geophys. Res.*, 81, 1976, pp. 245-252.

13. Walker, R. J., K. N. Erickson, R. L. Swanson, and J. R. Winckler, "Substorm Associated Particle Boundary Motion at Synchronous Orbit," (Abstract), *EOS: Transactions of the American Geophysical Union*, **56**(1), 1975, p. 422.

14. Svalgaard, L., *An Atlas of Interplanetary Sector Structure 1957-1974*, Stanford University Institute for Plasma Research Report 629, June 1975.

15. Russell, C. T., "The Solar Wind and Magnetospheric Dynamics," in *Correlated Interplanetary and Magnetospheric Observations*, D. E. Page, ed., D. Reidel Publishing Co., Dordrecht, Holland, 1974, pp. 3-47.

16. Fritz, T. A., and B. Wilken, "Substorm Generated Fluxes of Heavy Ions at the Geostationary Orbit," in *Magnetospheric Particles and Fields*, B. M. McCormac, ed., D. Reidel Publishing Co., Dordrecht Holland, 1976, pp. 171-179.

17. DeForest, S. E., "Spacecraft Charging at Synchronous Orbit," *J. Geophys. Res.*, 77(4), 1972, pp. 651-659.

18. Whipple, E. C., Jr., "Observation of Photoelectrons and Secondary Electrons Reflected from a Potential Barrier in the Vicinity of ATS-6," *J. Geophys. Res.*, 81(4), 1976, pp. 715-720.

19. Whipple, E. C., Jr., "Theory of the Spherically Symmetric Photoelectron Sheath: A Thick Sheath Approximation and Comparison with the ATS-6 Observation of a Potential Barrier," *J. Geophys. Res.*, 81(4), 1976, pp. 601-607.

1. Report No. TP-1101	2. Government Accession No.	3. Recipient's Catalog No.
4. Title and Subtitle Significant Initial Results from the Environmental Measurements Experiment on ATS-6		5. Report Date December 1977
		6. Performing Organization Code 410
7. Author(s) T. A. Fritz, J. P. Corrigan, et al.		8. Performing Organization Report No. G-7702 F-15
9. Performing Organization Name and Address Goddard Space Flight Center Greenbelt, Maryland 20771		10. Work Unit No. 385-36-02
		11. Contract or Grant No.
12. Sponsoring Agency Name and Address National Aeronautics and Space Administration Washington, D.C. 20546		13. Type of Report and Period Covered Technical Paper
		14. Sponsoring Agency Code

15. Supplementary Notes

16. Abstract

The Applications Technology Satellite (ATS-6), launched into synchronous orbit on May 30, 1974, carried a set of six particle detectors and a triaxial fluxgate magnetometer. The particle detectors are able to determine the ion and electron distribution functions from 1 to greater than 10^8 eV. Significant initial results include the following:

The magnetic field is weaker and more tilted than predicted by models which neglect internal plasma. There is also a seasonal dependence to the magnitude and tilt. ATS-6 magnetic-field measurements show the effects of field-aligned currents associated with substorms, and large fluxes of field-aligned particles are observed with the particle detectors.

Encounters with the plasmasphere reveal the existence of warm plasma with temperatures up to 30 eV. A variety of correlated waves in both the particles and fields are observed: pulsation contin-uous (Pc)1 oscillations, seen predominantly in the plasmasphere bulge; ultralow frequency (ULF) standing waves; ring current proton ULF waves; and low frequency waves that modulate the ener-getic (50 to 1000 keV) electrons. In addition, large-scale waves on the energetic-ion-trapping boundary are observed, and the intensity of energetic electrons is modulated in association with the passage of sector boundaries of the interplanetary magnetic field. Heavy ions that are probably oxygen sometimes dominate the energetic-ion population. Finally, differential charging of the space-craft appears to dominate the local electrostatic potential distribution.

17. Key Words (Selected by Author(s)) ATS-6, Magnetometer, Proton, Electron, Ion, Plasmasphere, Potential, Charging, Electrostatic, Synchronous, EME	18. Distribution Statement Unclassified—Unlimited		
19. Security Classif. (of this report) Unclassified	20. Security Classif. (of this page) Unclassified	21. No. of Pages 34	22. Price* $4.50

14   1 1U,E,   121277 S00903DS
DEPT OF THE AIR FORCE
AF WEAPONS LABORATORY
ATTN: TECHNICAL LIBRARY (SUL)
KIRTLAND AFB NM 87117

NASA